

4. SITE 1269¹

Shipboard Scientific Party²

OPERATIONS SUMMARY

Transit to Site 1269

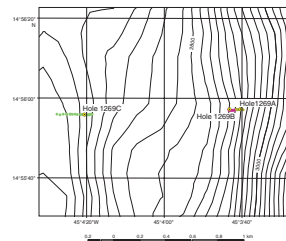
Using the ship's dynamic positioning system, we moved ~5 nmi to Site 1269 (Fig. F1). During the move a two-stand bottom-hole assembly was built consisting of six 8.25-in drill collars. This was done to minimize the risk of losing additional drill collars and jeopardizing further operations. As at Site 1268, all collars were inspected before inclusion in the drill string.

Hole 1269A

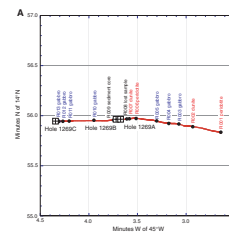
Prior to initiating Hole 1269A, we undertook a 1.25-hr subsea camera survey to verify our location as compared to site survey videotapes. The drilling target for Site 1269 was along the track of *Shinkai* 6500 submersible Dive 423 in 1998, which recovered samples of peridotite and gabbro from a series of steep outcrops separated by flat, sedimented seafloor along the western flank of the Mid-Atlantic Ridge axial valley. Our camera survey for Hole 1269A began at a depth where the site survey dive had recovered dunite (*Shinkai* 6500 Dive 423, sample R007) (Fig. F2). After moving downslope 60 m to ensure we were above an outcrop and in sediment free of talus, we released a positioning beacon from the camera frame 30 m east of our selected drilling target, retrieved the camera, and spudded Hole 1269A.

Hole 1269A was initiated at 1005 hr on 27 May 2003 with a seafloor tag depth of 2809 meters below sea level (mbsl). Coring continued to a depth of 15.3 meters below seafloor (mbsf) (Table T1) before high drilling torque, collapsing hole, and low recovery (2.6%) consisting of only fragments of basalt led us to terminate coring. At 1425 hr on 27 May the bit cleared the seafloor, ending Hole 1269A.

F1. Bathymetry and survey tracks, p. 7.



F2. Track of *Shinkai* Dive 423, hole location, and bathymetric section of Site 1269, p. 8.



T1. Coring summary, p. 14.

¹Examples of how to reference the whole or part of this volume.

²Shipboard Scientific Party addresses.

Hole 1269B

Our second subsea camera survey at Site 1269 began with the drill pipe over the positioning beacon. We surveyed 60 m west, continuing along a flat, sedimented seafloor, free of talus shed from uphill. A push-in test indicated the sediment was <5 m thick, so we retrieved the camera and spudded Hole 1269B.

At 1950 hr on 27 May, Hole 1269B was initiated with a seafloor tag depth of 2799 mbsl. The first core was recovered after 11.1 m of penetration and again contained only a few pieces of basalt. As in Hole 1269A, high torque and recovery of only basalt fragments suggested we would not reach our drilling objectives without first drilling through an unknown thickness of unstable basaltic lava, so we abandoned the hole. The bit cleared the seafloor at 2215 hr on 27 May, ending Hole 1269B. Anticipating a move of ~1 km, we recovered the positioning beacon.

Hole 1269C

With two holes at our most promising target yielding only basalt, we elected to move farther uphill (west) for our next hole at Site 1269. After offsetting the drill ship ~1.1 km west, we conducted our third subsea camera survey at this site. This location was near the top of the western rift valley wall, in a flat, sedimented terrain above a moderate slope from which four samples of gabbro were collected during *Shinkai* 6500 Dive 423 (Fig. F2). After surveying 275 m upslope, we returned to a position ~65 m west of the start of our camera survey to begin Hole 1269C (Fig. F1).

Hole 1269C was initiated at 1118 hr on 28 May. Coring was again hampered by high and erratic torque, and the two core barrels (to a depth of 18.3 mbsf) that were recovered contained only a few fragments of basalt. Recognizing that our favored drilling targets at Site 1269 were all covered with a basaltic carapace beneath a few meters of pelagic sediment, we elected to terminate coring at this site and to move to one of our alternate sites. The drill string and positioning beacon were recovered, and we completed operations at Site 1269 at 2000 hr on 28 May.

IGNEOUS AND MANTLE PETROLOGY

Lithology

Except for Sections 209-1269B-1R-1 (Piece 1) and 209-1269C-1R-1 (Pieces 3–5), all pieces from Holes 1269A, 1269B, and 1269C are small, nonoriented, and composed of rather fresh porphyritic to aphyric basalt. Phenocrysts in basalt include olivine and plagioclase with minor amounts of clinopyroxene and spinel. The texture is glomerocrystic in some basalts from Holes 1269A and 1269B. A sector of pillow basalt with variolitic structure toward the rim that includes a few chips of fresh glass is found in Section 209-1269C-1R-1 (Piece 1). Vesicles make up >15% of the volume in some basalt from Holes 1269B and 1269C.

The black vesicular basalts drilled in Holes 1269A, 1269B, and 1269C are essentially unaltered. Locally, olivine phenocrysts are slightly oxidized and one clay + iron oxyhydroxide veinlet with an irregular green-

ish gray halo was observed in Hole 1269C at 0.12 mbsf. The basalts are not deformed and display no structural features.

None of the core sections display high natural gamma radiation or magnetic susceptibility. The mean magnetic susceptibilities of cores from Holes 1269A and 1269B are $222 \pm 85 \times 10^{-5}$ and $177 \pm 92 \times 10^{-5}$ SI, respectively.

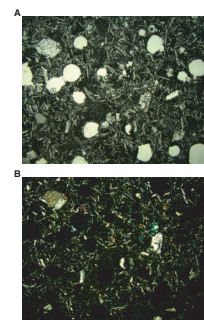
Microcrystalline intersertal to intergranular textures (Fig. F3) are present in thin sections of two basalts (Samples 209-1269B-1R-1, 2–5 cm, and 1R-1, 44–46 cm). Acicular plagioclase laths and quench clinopyroxene with minor amounts of fresh brown glass and skeletal opaque minerals make up the groundmass. The fine-grained, branching clinopyroxene crystals are indicative of relatively rapid quenching (Fig. F4). Some large spinel phenocrysts (<0.8 mm) have melt inclusions and/or inclusions of other minerals. Small euhedral to subhedral spinel grains are also included within olivine and plagioclase phenocrysts.

Vesicle Size Distribution

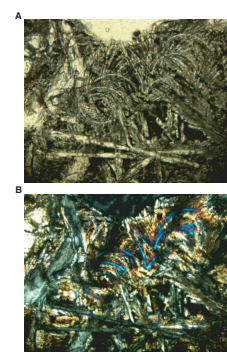
Mid-ocean-ridge basalt (MORB) erupted below 2500 m water depth typically has vesicularities (volume fraction of vesicles) of 1%–2% due to the large hydrostatic pressure (Moore et al., 1977). The 14°–15°N section of the Mid-Atlantic Ridge is an area where relatively high volatile contents in basalts have been observed (e.g., Staudacher et al., 1989; Javoy and Pineau, 1991). Rare examples of “popping rocks” with very high carbon dioxide contents and unique noble gas characteristics were recovered from this region (Staudacher et al., 1989; Sarda and Graham, 1990; Javoy and Pineau, 1991; Burnard et al., 1997; Moreira et al., 1998). Popping rocks are peculiar samples notable for their active popping on the ship’s deck soon after recovery from the seafloor as their trapped gases are rapidly released (Hekinian et al., 1973; Pineau et al., 1976). We studied the vesicle size distribution of two basalts from Hole 1269B (intervals 209-1269B-1R-1 [Piece 1, 0–8 cm] and 1R-1 [Piece 7, 39–47 cm]) using digital image analysis. The vesicularity for these two basalts is very similar to that for the 14°N popping rocks (~16%) (Sarda and Graham, 1990).

The theory and application of crystal size distribution is now an active area of study in igneous petrology (e.g., Marsh, 1988, 1998; Cashman, 1993). Although vesicle size distribution (VSD) studies of basalts reveal important clues about magma dynamics and the style of degassing (e.g., Cashman et al., 1994; Mangan and Cashman, 1996), there have been only a few such studies and only one on MORB (Sarda and Graham, 1990). For two Hole 1269B basalts, digital photo images from the split core face were imported into an image analysis program (NIH Image, version 1.63) and the sizes of all vesicles were determined. These images were edited to separate “touching particles” that could clearly be discerned as individual bubbles and to remove “digital noise.” Image resolution was 100 pixels/mm². We used a minimum threshold of 3 pixels for the area of particles. From the particle areas we calculated individual bubble diameters assuming spherical geometry. A comparison of digital images of the two core samples with this idealized model derived from the computer image processing is shown in Figure F5. The vesicle size results were then binned logarithmically according to their diameter, beginning at the largest size of 2.23 mm observed in Piece 7 and 2.17 mm in Piece 1. The total number of objects having diameters between 2.2 and 0.2 mm counted by this procedure were 729 and 843 for Pieces 1 and 7, respectively. The number of vesicles in each size class

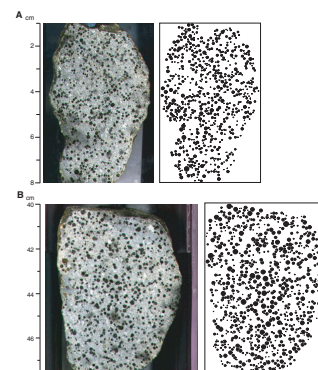
F3. Typical vesicular basalt, p. 10.



F4. Plagioclase, glass, and quench clinopyroxene crystals, p. 11.



F5. Photographs and binary images of bubble size distribution, p. 12.



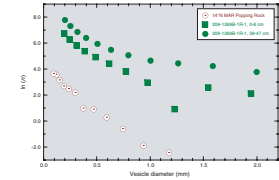
was converted to number per unit volume (N_v), following the Saltykov method for stereological analysis as outlined in Sarda and Graham (1990). The population density (n) is N_v divided by the bin width and has the units of cm^{-4} . The results are displayed on a diagram of the logarithm of population density vs. vesicle diameter in Figure F6, where they are also compared to the earlier popping rock results.

The modal percent vesicles for these two Hole 1269B basalts determined from the image analysis are very similar (Piece 1 = 15.2% and Piece 7 = 16.2%). Both also display curved VSDs. This VSD shape has several possible origins, related to variations in nucleation and growth rates of bubbles (Marsh, 1998). Piece 7 could also be described as a “kinked” VSD, having two quasi-linear intervals (0.8–1.5 and 0.3–0.7 mm). Such kinked patterns are found in crystals from historical eruptions at Mt. Etna and were suggested to reflect changes in nucleation and growth during the transition from magma storage to ascent (Armenti et al., 1994). By analogy to the Etna study, the larger vesicles (~0.8–1.5 mm) in Piece 7 may reflect bubble nucleation and growth deeper in the magma plumbing system. In comparison, the smaller (0.3–0.7 mm) vesicles may have formed during later stages of magma ascent and eruption. In contrast, Piece 1, which also shows a curved VSD, has a notable deficiency of vesicles in the size class centered around 1.23 mm. This pattern may be produced by coalescence of smaller bubbles (Marsh, 1998). At small bubble sizes (0.3–0.7 mm) this second sample has a slope similar to that for Piece 7. Intriguingly, the slope at small bubble sizes for both samples is similar to that for the 14°N popping rock (approximately -5.5). This popping rock has been interpreted, on the basis of its VSD, relative abundance of rare gas, and high CO_2 content, to represent a rare case of undegassed MORB (Sarda and Graham, 1990). The relative positions on the VSD diagram of the two basalts and the popping rock may represent a temporal evolutionary pattern similar to what has been described for crystals in volcanic rocks. Marsh (1998) demonstrated that the negative log-linear slope of natural crystal size distributions is consistent with nucleation and growth in a system in which nucleation rate increases with time. This produces a VSD that migrates systematically up the $\ln(n)$ axis and across the size (D) axis at a rate that is determined by the bubble growth rate. Following this reasoning, the three cases shown in Figure F6 might be viewed as snapshots of maturing bubble systems in MORB with the popping rock representing the most primitive system and Sections 209-1269B-1R-1 (Pieces 1 and 7) representing more evolved systems.

MICROBIOLOGY

Mud samples were collected from Holes 1269A and 1269C for microbial analysis. Samples were taken from sediment recovered from the core barrel after a push-in test with the drill bit to determine sediment thickness. Microscopic observation showed that the samples were composed of nannofossils and fine inorganic particulates. Because no mudline was established, no sample designation was assigned beyond hole number. From Holes 1269A and 1269C, 9.0 and 18.3 g of reddish brown mud were collected, respectively. Direct counts and culture of the samples were prepared as described in “Microbiology,” p. 24, in the “Explanatory Notes” chapter and Table T2. As no bacteria were observed in the Hole 1269A sample, 10 μL of the cleared artificial seawater was used to prepare a dilution series to 10^{-7} , and 100 μL of each dilution

F6. Population density vs. vesicle diameter, p. 13.



T2. Microbiology data for mud samples, p. 15.

spread was plated onto nutrient agar and incubated at room temperature. No growth was observed on any of the plates after 72 hr of incubation. When no growth was noted at 24 hr of incubation, both samples (from Holes 1269A and 1269C) were again mixed by shaking until the mud sediments were in solution. Ten microliters from each sample (no clearing allowed) was added to 900 μ L of artificial seawater and spread over a 45-mm nitrocellulose membrane filter that had been placed on nutrient agar plates. Excess water was aspirated off the filters with a pipette, leaving the sediment particles on the filter surface. Growth was noted on both plates at 24 hr, indicating that the bacteria in the samples were predominantly associated with sediments.

REFERENCES

- Armienti, P., Pareschi, M.T., Innocenti, F., and Pompilio, M., 1994. Effects of magma storage and ascent on the kinetics of crystal growth: the case of the 1991–93 Mt. Etna eruption. *Contrib. Mineral. Petrol.*, 115:402–414.
- Burnard, P., Graham, D., and Turner, G., 1997. Vesicle-specific noble gas analyses of “popping rock”: implications for primordial noble gases in Earth. *Science*, 276:568–571.
- Cashman, K.V., 1993. Relationship between plagioclase crystallization and cooling rate in basaltic melts. *Contrib. Mineral. Petrol.*, 113:126–142.
- Cashman, K.V., Mangan, M.T., and Newman, S., 1994. Surface degassing and modifications to vesicle size distributions in Kilauea basalt. *J. Volcanol. Geotherm. Res.*, 61:45–68.
- Fujiwara, T., Lin, J., Matsumoto, T., Kelemen, P.B., Tucholke, B.E., and Casey, J., 2003. Crustal evolution of the Mid-Atlantic Ridge near the Fifteen-Twenty Fracture Zone in the last 5 Ma. *Geochem. Geophys. Geosyst.*, 4:10.1029/2002GC000364.
- Hekinian, R., Chaigneau, M., and Cheminée, J.-L., 1973. Popping rocks and lava tubes from the Mid-Atlantic Rift Valley at 36°N. *Nature*, 245:277.
- Javoy, M., and Pineau, F., 1991. The volatiles record of a “popping” rock from the Mid-Atlantic Ridge at 14°N: chemical and isotopic composition of gas trapped in the vesicles. *Earth Planet. Sci. Lett.*, 107:598–611.
- Mangan, M.T., and Cashman, K.V., 1996. The structure of basaltic scoria and reticulate and inferences for vesiculation, foam formation, and fragmentation in lava fountains. *J. Volcanol. Geotherm. Res.*, 73:1–18.
- Marsh, B.D., 1988. Crystal size distribution (CSD) in rocks and the kinetics and dynamics of crystallization, I: Theory. *Contrib. Mineral. Petrol.*, 99:277–291.
- , 1998. On the interpretation of crystal size distributions in magmatic systems. *J. Petrol.*, 39:553–599.
- Moore, J.G., Batchelder, J.N.N., and Cunningham, C.G., 1977. CO₂ filled vesicles in mid-ocean ridge basalts. *J. Volcanol. Geotherm. Res.*, 2:309–374.
- Moreira, M., Kunz, J., and Allègre, C., 1998. Rare gas systematics in popping rock: isotopic and elemental compositions in the upper mantle. *Science*, 279:1178–1181.
- Pineau, F., Javoy, M., and Bottinga, Y., 1976. ¹³C/¹²C ratios of rocks and inclusions in popping rocks of the Mid-Atlantic Ridge and their bearing on the problem of isotopic composition of deep-seated carbon. *Earth Planet. Sci. Lett.*, 29:413–421.
- Sarda, P., and Graham, D., 1990. Mid-ocean ridge popping rocks: implications for degassing at ridge crests. *Earth Planet. Sci. Lett.*, 97:268–289.
- Staudacher, T., Sarda, P., Richardson, S.H., Allegré, C.J., Sagna, I., and Dimitriev, L.V., 1989. Noble gases in basalt glasses from a Mid-Atlantic Ridge topographic high at 14°N: geodynamic consequences. *Earth Planet. Sci. Lett.*, 96:119–133.

Figure F1. Bathymetric map with subsea camera survey tracks plotted. Bathymetric data courtesy of T. Fujiwara and T. Matsumoto of JAMSTEC (Fujiwara et al., 2003).

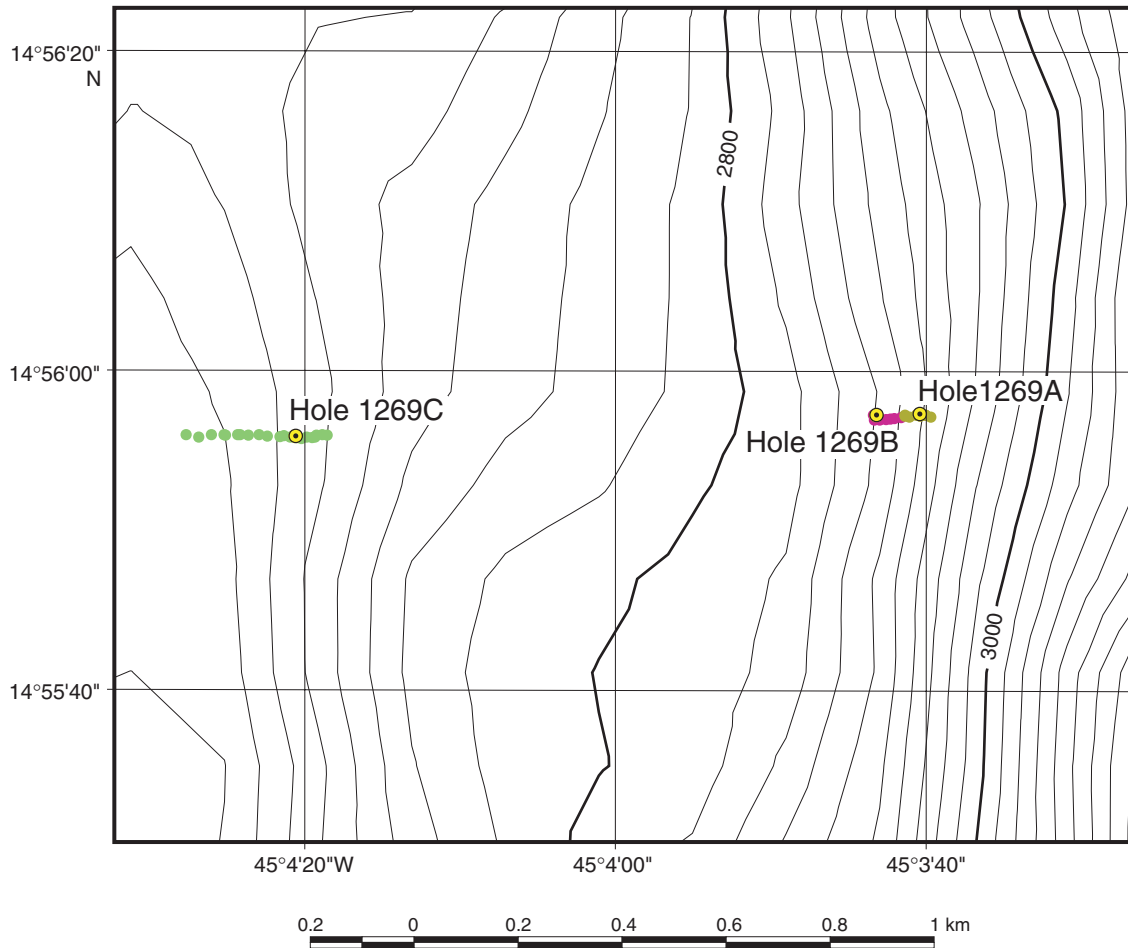


Figure F2. A. Location map with track of *Shinkai* 6500 Dive 423, locations and lithologies of samples from that dive, and the approximate positions along the dive track of Holes 1269A, 1269B, and 1269C. (Continued on next page.)

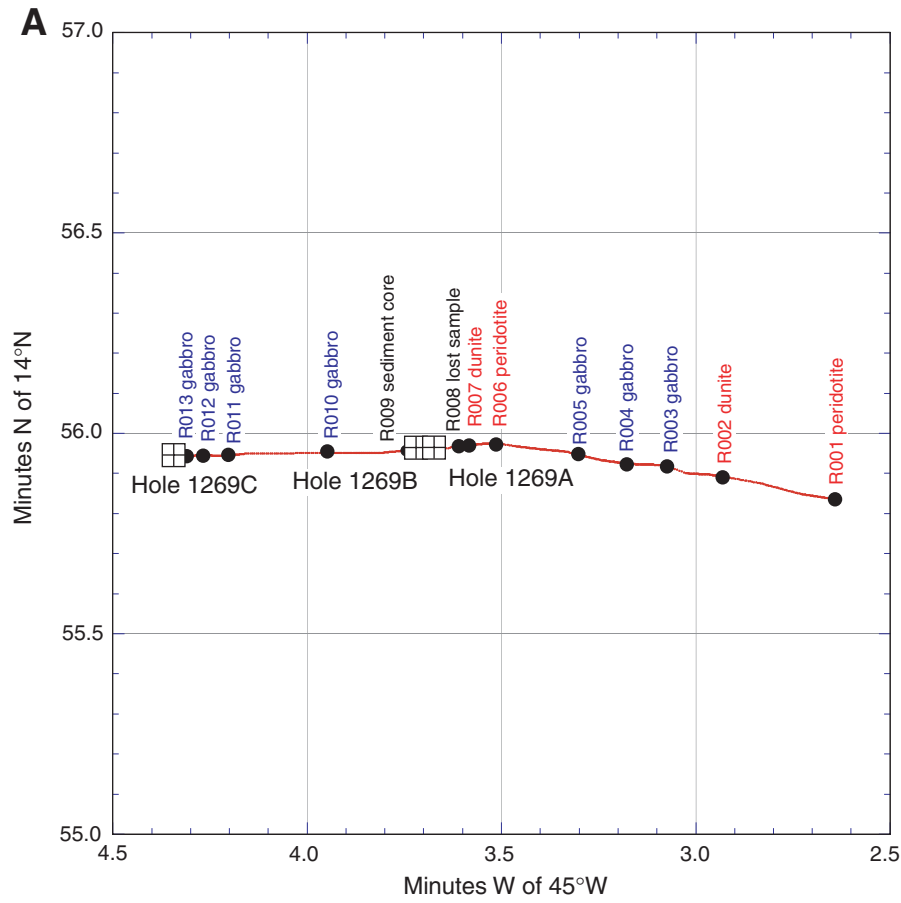


Figure F2 (continued). B. Bathymetric section based *Shinkai* 6500 Dive 423, projected along 264° with no vertical exaggeration. Locations and lithologies of samples collected during the dive, as well as the approximate positions of Holes 1269A, 1269B, and 1269C are indicated.

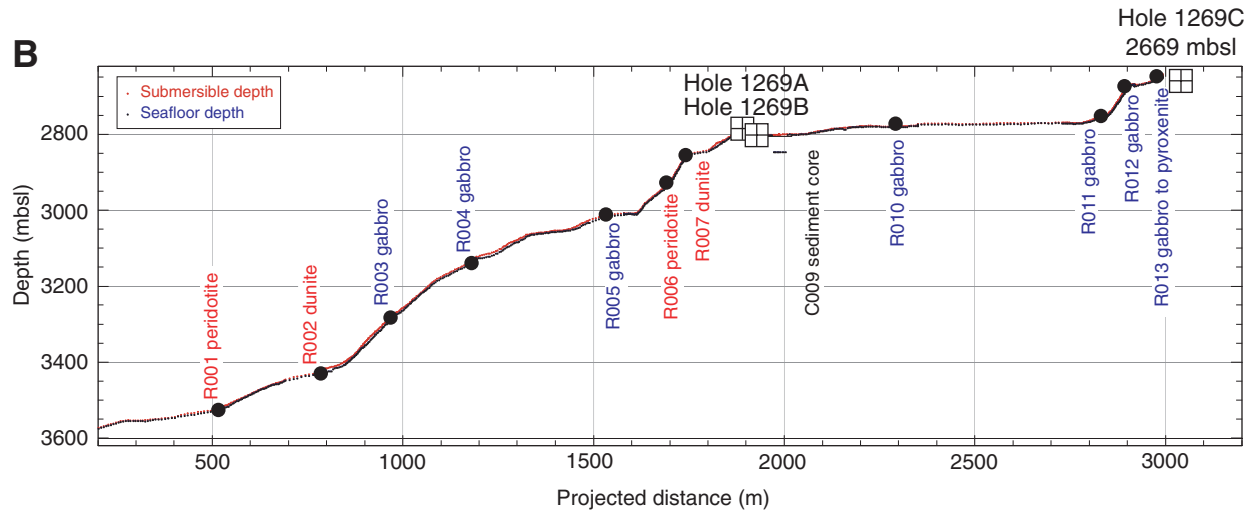
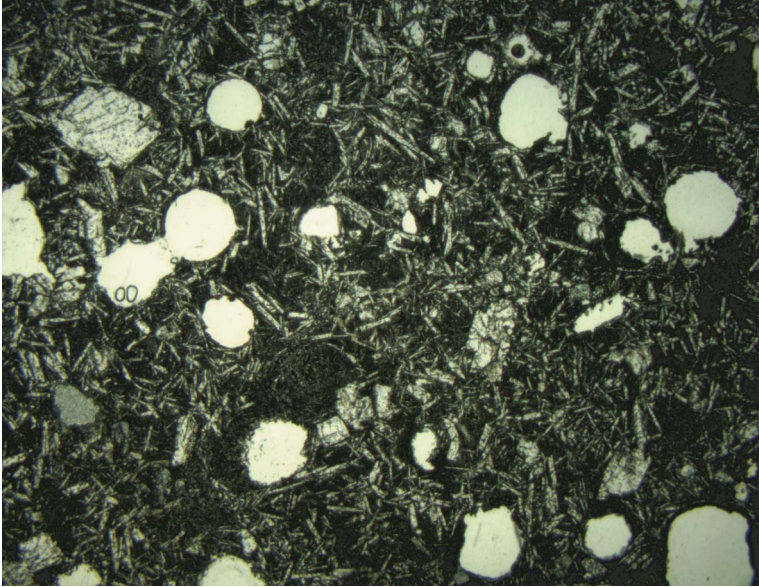


Figure F3. Photomicrographs showing typical vesicular basalt (Sample [209-1269B-1R-1 \[Piece 7, 44–46 cm\]](#)) (blue filter; field of view = 11 mm). A. Plane-polarized light; image 1269B_001. B. Cross-polarized light; image 1269B_002.

A



B

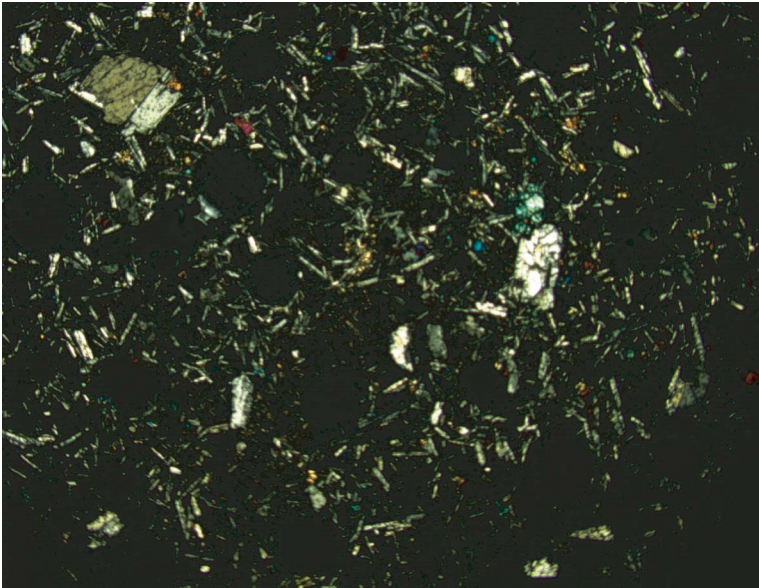
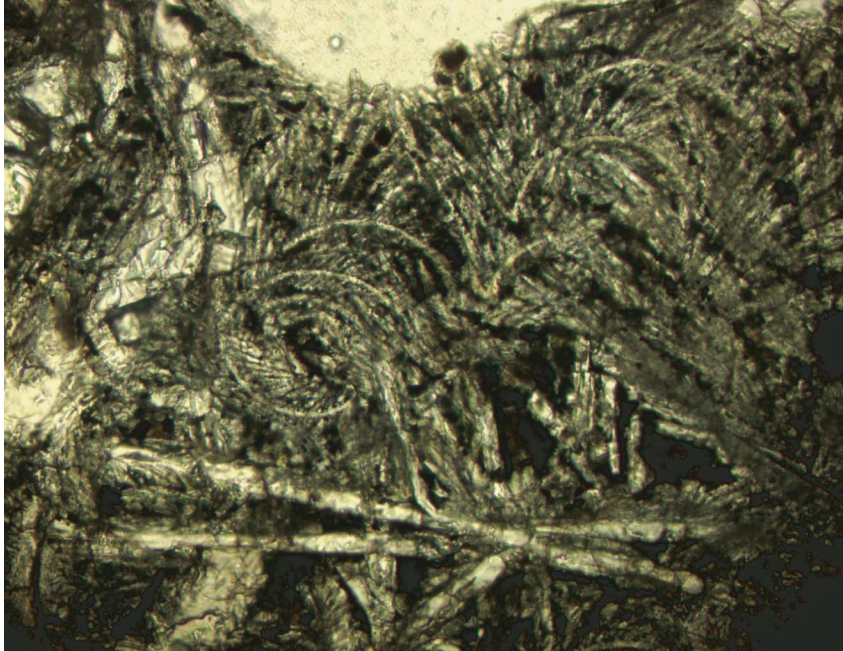


Figure F4. Photomicrographs showing plagioclase, glass, and quench clinopyroxene crystals in ground-mass. Note the spinel phenocryst in the upper right corner (Sample 209-1269B-1R-1 [Piece 7, 44–46 cm]). A. Plane-polarized light: blue + gray filters; field of view = 0.7 mm; image 1269B_003. B. Cross-polarized light: blue filter; field of view = 0.7 mm; image 1269B_004.

A



B

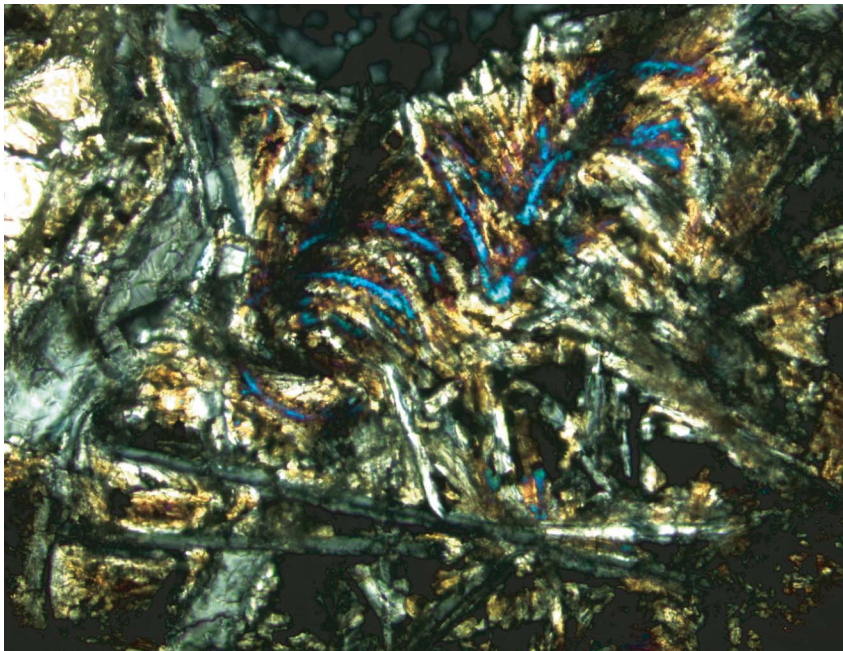


Figure F5. Comparison of the photographic images and the idealized binary images of bubble size distribution produced by computer analysis. A. Sample 209-1269B-1R-1, 0–8 cm. B. Sample 209-1269B-1R-1, 39–47 cm.

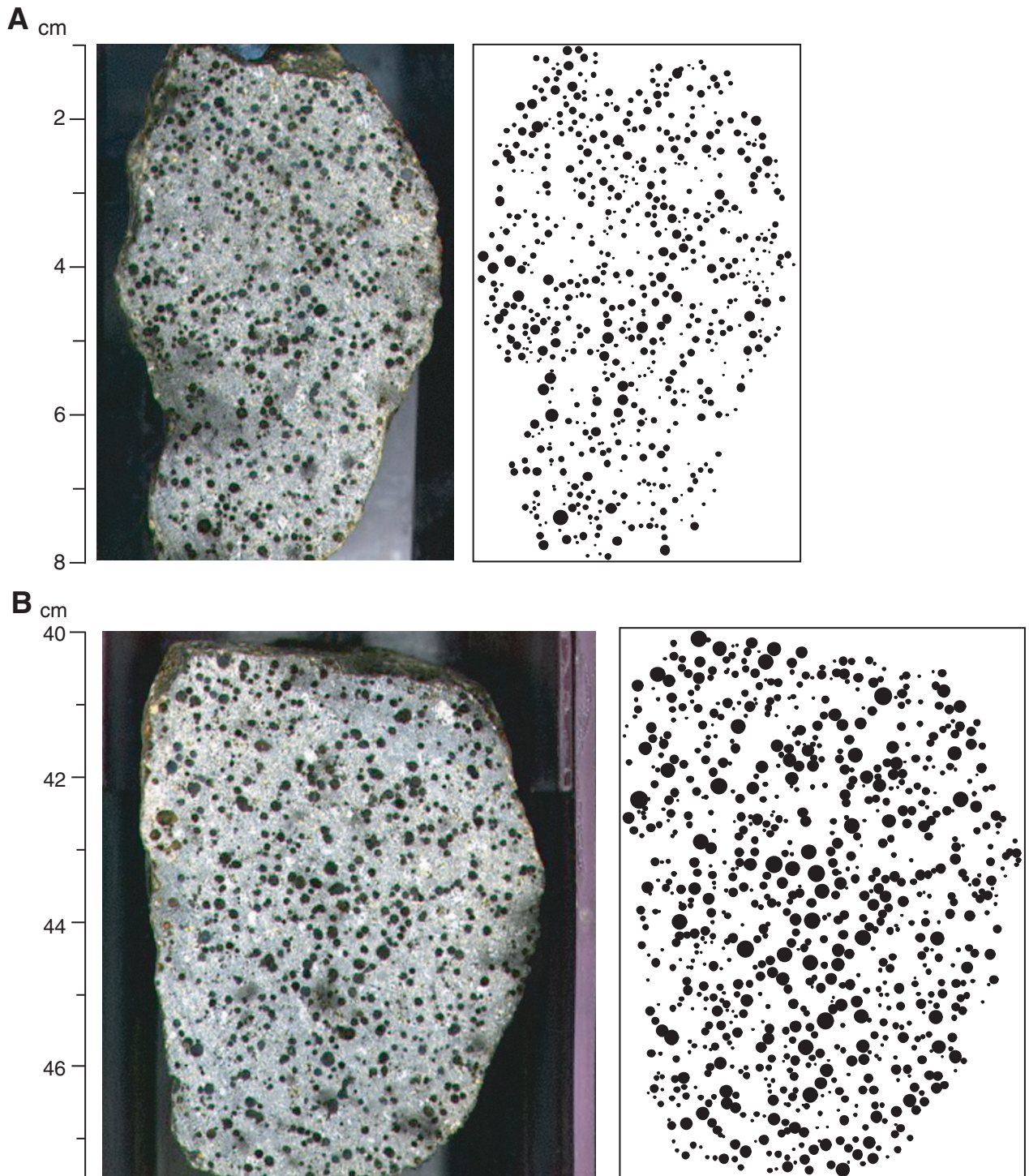


Figure F6. Population density vs. vesicle diameter for the two samples analyzed from Hole 1269B compared to the popping rock results of Sarda and Graham (1990). MAR = Mid-Atlantic Ridge.

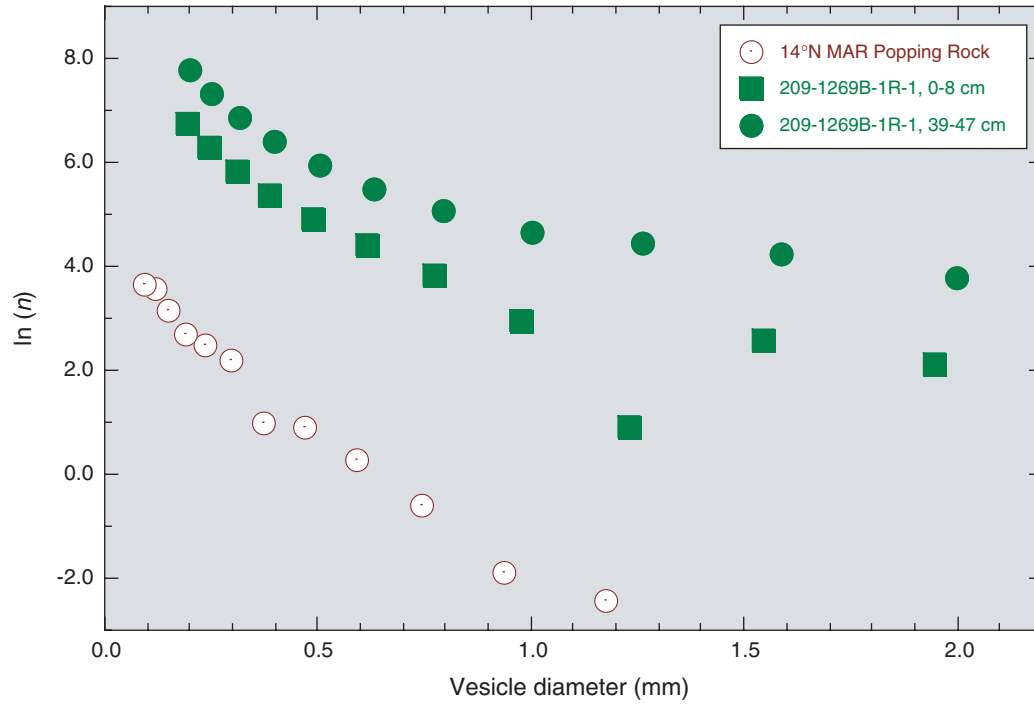


Table T1. Coring summary, Site 1269.

Hole 1269A

Latitude: 14°55.9632'N
 Longitude: 45°03.6734'W
 Time on site: 48.50 (1930 hr, 26 May–2000 hr, 28 May 2003)
 Time on hole: 19.00 (1930 hr, 26 May–1430 hr, 27 May 2003)
 Seafloor (drill pipe measurement from rig floor, mbrf): 2820.0
 Distance between rig floor and sea level (m): 11.0
 Water depth (drill pipe measurement from sea level, m): 2809.0
 Total depth (drill pipe measurement from rig floor, mbrf): 2835.3
 Total penetration (mbsf): 15.3
 Total length of cored section (m): 15.3
 Total core recovered (m): 0.39
 Core recovery (%): 2.55
 Total number of cores: 1

Hole 1269B

Latitude: 14°55.9620'N
 Longitude: 45°03.7205'W
 Time on hole: 7.75 (1430 hr, 27 May–2215 hr, 27 May 2003)
 Seafloor (drill pipe measurement from rig floor, mbrf): 2810.5
 Distance between rig floor and sea level (m): 11.0
 Water depth (drill pipe measurement from sea level, m): 2799.5
 Total depth (drill pipe measurement from rig floor, mbrf): 2821.6
 Total penetration (mbsf): 11.1
 Total length of cored section (m): 11.1
 Total core recovered (m): 0.53
 Core recovery (%): 4.8
 Total number of cores: 1

Hole 1269C

Latitude: 14°55.9401'N
 Longitude: 45°04.3435'W
 Time on hole: 21.75 (2215 hr, 27 May–2000 hr, 28 May 2003)
 Seafloor (drill pipe measurement from rig floor, mbrf): 2678.5
 Distance between rig floor and sea level (m): 11.0
 Water depth (drill pipe measurement from sea level, m): 2667.5
 Total depth (drill pipe measurement from rig floor, mbrf): 2696.8
 Total penetration (mbsf): 18.3
 Total length of cored section (m): 18.3
 Total core recovered (m): 0.26
 Core recovery (%): 1.42
 Total number of cores: 2

Core	Date (May 2003)	Local time (hr)	Depth (mbsf)		Length (m)		Recovery (%)	
			Top	Bottom	Cored	Recovered		
209-1269A-								
1R	27	1520	0.0	15.3	15.3	0.39	2.6	
					Cored total:	15.3	0.39	2.6
209-1269B-								
1R	27	2310	0.0	11.1	11.1	0.53	4.8	
					Cored total:	11.1	0.53	4.8
209-1269C-								
1R	28	1305	0.0	12.3	12.3	0.11	0.9	
2R	28	1410	12.3	18.3	6.0	0.15	2.5	
					Cored totals:	18.3	0.26	1.4

Table T2. Microbiology data for mud, Holes 1269A and 1269C.

Hole	Depth (mbsl)	Date (May 2003)	Bacteria (counts/mL)	Viruses (counts/mL)	Bacteria culture (CFU/g)
1269A	2810	27	0	2.10×10^6	1.39×10^7
1269C	2668	28	6.03×10^4	9.81×10^4	1.08×10^7

Note: CFU = colony-forming units. This table is also available in [ASCII](#).